CHAPTER 93

A Boussinesq breaking wave model with vorticity

I. A. Svendsen, Ke Yu, and J. Veeramony[1]

ABSTRACT: The paper describes a breaking wave model based on the classical assumptions for long, moderately nonlinear Boussinesq waves. It is shown that wave breaking can be described by accounting for the effect of vorticity generated by the breaking process. This leads to two additional terms in the momentum equation, both of which represent the enhancement of the momentum flux associated with the extra particle velocities found at and around the turbulent front of the breaking waves. In addition to the wave height decay and profile deformation predicted by earlier breaker models, the present model also provides information about particle velocity profiles including the undertow. Comparisons are made to measurements for these quantities. The similarities and differences between various breaker models are also examined and explained.

1. Introduction

The present paper presents a Boussinesq wave model that includes the effects of wave breaking in the equation of continuity and momentum.

The process of wave breaking has been widely studied during particularly the past two decades. For a long time, almost all detailed information came from experimental investigations but the success of the Boussinesq approach in modelling nearshore wave motion has also lead to Boussinesq models that, by various means, create the decrease in wave height and the transformation of the wave shape observed during breaking in the surf-zone on a gently sloping beach.

Since breaking involves strong energy dissipation, it was natural as a first approach to heuristically add a "dissipation term", usually taking the form of the double derivative of the unknown variable to the momentum equation. Early examples are Zelt (1991), Karambas et al (1992) and more have followed. If the coefficient for the dissipation term is chosen carefully as in Wei et al (1995), such models can give breaker like wave development. The reason for this will be discussed later.

However, the Boussinesq wave models are developed from the fundamental equations of hydrodynamics. In the case of wave breaking this would mean the

[1]Center for Applied Coastal Research, Ocean Engineering Lab, University of Delaware, Newark, DE 19716, USA. Correspondence e-mail: ias@coastal.udel.edu

Reynolds equations, in which the Reynolds stresses represent the only signature of the turbulence generated by breaking. Following the usual procedure, one finds (if the Reynolds stresses, as a reasonable approach, are modelled by means of an eddy viscosity) that the "dissipation term" of the assumed $\partial^2/\partial x^2$-form originates from the turbulent normal stresses, which are small (see eg. Stive and Wind, 1982) and are very far from modelling the dramatic changes in the momentum flux typical of wave breaking.

An approach closer to meet that goal was used by Brocchini et al (1992) and, in more explicit form, by Schäffer et al (1992, 1993). They observed the importance the roller of a mature breaking wave has in enhancing the momentum flux of the wave. The roller essentially is the volume of recirculating water flow carried forward in the turbulent front at the speed c of the wave. The concept was first used by Svendsen (1984a,b) in the wave averaged equations to calculate wave height decay, set-up and undertow. The two above mentioned models essentially introduced that concept into the Boussinesq equations, and, though there are limitations, the results are remarkably convincing, as they should be because the models give an approximate representation of the actual physics. In addition, such models only represent a moderate extension of the computational work relative to Boussinesq models for non-breaking waves.

Because of the heuristically assumed form of the velocity profiles, these models cannot be expected to provide detailed information about the particle motion in the breaking wave motion, including the undertow. The model presented in the following is aiming at including such information by avoiding apriori assumptions about the velocity profiles. This means it is necessary to include in the model the vorticity generated by the breaking, which is an important feature of breaking waves: the motion is not irrotational as assumed in traditional Boussinesq theory.

The model is therefore formulated in terms of a stream function and the vorticity is an additional unknown which is determined separately by solving the vorticity transport equation. The model equations are outlined in section 2 and section 3 gives additional discussion about particularly the boundary conditions for the vorticity. In section 4 we show a comparison with measurements including particle velocities and undertow. The last section gives a comparison with previous models mentioned above which explains why all these models seem equally successful in predicting the wave height and wave profile development.

2. Outline of model equations

The governing equations are derived from the basic equations for conservation of mass and momentum. Only a brief outline is given here, for more details see Yu & Svendsen, 1995. We consider a breaking wave propagating over a gently sloping bottom topography of depth $h_0(x)$. Fig 1 shows the definitions of all geometrical quantities used. Then the depth integrated equations of continuity and momentum becomes

$$\frac{\partial \zeta}{\partial t} + \frac{\partial Q}{\partial x} = 0 \tag{1}$$

where

$$Q = \int_{-h_0}^{\zeta} u dz \tag{2}$$

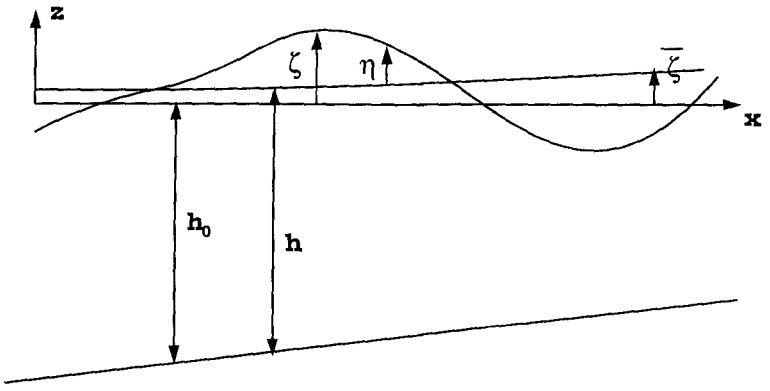

Figure 1: Definition sketch showing the geometrical quantities.

and

$$\frac{\partial Q}{\partial t}+\frac{\partial}{\partial x}\int_{-h_0}^{\zeta}u^2dz-(h_0+\zeta)\frac{\partial\zeta}{\partial x}-\int_{-h_0}^{\zeta}\frac{\partial^3}{\partial x^2\partial t}\int_z^{\zeta}\int_{-h_0}^{z}udzdzdz$$
$$-\int_{-h_0}^{\zeta}\frac{\partial^2}{\partial x^2}\int_z^{\zeta}u\frac{\partial}{\partial x}\int_{-h_0}^{z}udzdzdz+\frac{\tau_b-\tau_s}{\rho}=0 \qquad (3)$$

where τ_b and τ_s are the bottom and surface stresses, respectively. In (3) the pressure term has been eliminated using the depth integrated vertical component of the momentum equation.

To evaluate the integrals in (3) the velocity u must be determined. In breaking waves the flow cannot be assumed irrotational. However the stream function ψ for the flow satisfies the equation

$$\nabla^2\psi=\omega \qquad (4)$$

where ω is the vorticity which must be determined separately. Equation (4) is solved by introducing the usual assumptions of Boussinesq wave theory that the water depth to wave length ratio μ and wave amplitude to water depth ratio δ are small and δ/μ^2 are O(1). The stream function ψ can then be expanded in a power series

$$\psi=\sum_{n=0}^{\infty}(z+h_o)^n\psi_n(x,t) \qquad (5)$$

Substituting this into (4) and solving it turns out to be convenient to distinguish between the rotational and the irrotational part of the solution. Hence for the velocity we define u_r and u_p respectively and find

$$u_p=u_0-\mu^2(z+h_0)(2h_xu_{0x}+h_{xx}u_0)-\frac{\mu^2}{2}(z+h_0)^2u_{0xx}+O\left(\mu^4\right) \qquad (6)$$

$$u_r = \int_{-h_0}^{z} \omega dz - \mu^2 \int_{-h_0}^{z} \int_{-h_0}^{z} \int_{-h_0}^{z} \omega_{xx} dz dz + O\left(\mu^4,\ \mu^2 h_x,\ u^2 h_{xx}\right) \tag{7}$$

Though ω is assumed large, the ω_{xx} terms in (7) turn out to contribute little to the solution. The u_r-terms represent the additional terms generated by the presence of vorticity. We further define the discharge Q_r as

$$Q_r = \int_{-h_0}^{\zeta} u_r dz \tag{8}$$

which implies that $Q = Q_p + Q_r$.

When these results are substituted into the integrals of (3) these integrals can be written

$$\int_{-h_0}^{\zeta} u^2 dz = \frac{Q^2}{d} + \Delta M \tag{9}$$

$$\int_{-h_0}^{\zeta} \frac{\partial^3}{\partial x^2 \partial t} \int_{z}^{\zeta} \int_{-h_0}^{z} u dz dz dz = \frac{h^3}{6}\left(\frac{Q}{h}\right)_{xxt} - \frac{h^2}{2} Q_{xxt} + \Delta P_{xxt} \tag{10}$$

where $d = h_o + \zeta$ and again the ΔM and ΔP_{xxt} represent the contributions caused by the breaking. For ΔM and ΔP_{xxt} we get

$$\Delta M = \int_{-h_0}^{\zeta} u_r^2 dz - \frac{Q_r^2}{d} + O\left(\mu^4\right) \tag{11}$$

$$\Delta P = -\int_{-h}^{\bar{\zeta}} \int_{z}^{\bar{\zeta}} \int_{-h}^{z} u_r dz dz dz + \frac{\left(h + \bar{\zeta}\right)^2}{3} Q_{r\cdot} + O\left(\delta,\ \mu^2,\ h_x\right) \tag{12}$$

The Boussinesq equations for the breaking waves therefore become

$$\zeta_t + Q_x = 0 \tag{13}$$

$$Q_t + g\left(h_0 + \zeta\right)\zeta_x + \left(\frac{Q^2}{h}\right)_x + \Delta M_x + \frac{h^3}{6}\left(\frac{Q}{h}\right)_{xxt} - \frac{h^2}{2} Q_{xxt} + \Delta P_{xxt} = 0 \tag{14}$$

The two unknowns in these equations are the surface variation ζ and the total instantaneous volume flux Q in the waves. The vorticity ω is determined from the vorticity transport equation, which to the same order of approximation as (14) reads

$$\omega_t = [\nu_t \omega_z]_z + O(\mu^2, \delta) \tag{15}$$

where ν_t is the eddy viscosity. This is solved using the boundary conditions

$$\omega(-h) = 0 \tag{16}$$

$$\omega(\bar{\zeta}) = \omega_s \tag{17}$$

Here ω_s is the maximum value of ω generated near the surface due to the wave breaking.

3. Discussion of boundary conditions for the vorticity

The bottom boundary condition of zero vorticity is consistent with the general neglection of the bottom friction in the model.

At the free surface we can expect that the vorticity will be zero along the part of the surface which is outside the roller area.

In the roller region, the free surface vorticity will also be near zero. However, strong vorticity is generated inside the recirculating roller flow. Measurements in that region of breaking are not yet available for surf-zone conditions, but measurements have been made in weak hydraulic jumps (see Lin & Rockwell, 1994). The flow patterns in all such jumps will of course differ somewhat from breaking waves, in particular far away from the turbulent roller region. Around the roller region, however, the flows in a hydraulic jump and a surf-zone wave are very similar indeed with the same local mechanisms dominating. Hence the measurements around the roller in a hydraulic jump can be expected to model the equivalent conditions in a surf-zone wave well.

There are a number of flow features that play an important role in assessing the vorticity in this region. Considering a vertical section through a point in the roller, one of the dominating features observed in such measurements is the increase in vorticity to a maximum which always occurs at or below the so called dividing streamline, which is the streamline limiting the roller. Above that streamline, the average flow recirculates, below it continues to the downstream. At the toe of the turbulent region, the dividing streamline joins the surface streamline ahead of the jump.

In this region, we can approximate the vorticity ω by

$$\omega \sim \frac{\partial u}{\partial z} \tag{18}$$

and hence we notice that

$$\nu_t \omega \sim \frac{\tau_{zx}}{\rho} \tag{19}$$

Hence the specification of ν_t and ω_s is equivalent to the specification of the shear stress at the lower edge of the dividing streamline used in some breaker models (see eg. Brocchini et al, 1991 or Schäffer et al, 1992). The advantage of the present method, however is that through the solution of the vorticity transport equation, it explicitly models the mechanisms for the effect such a shear stress has on the entire flow, a problem previous models do not address at all.

In spite of the limited knowledge we have about the value of ω and ν_t, there are some very specific bounds on how these parameters vary. One such bound is given by (19). Fig 2 shows an analysis of the maximum shear stress which occurs at or just below the dividing streamline in three different hydraulic jumps with Froude numbers $F = 1.28$, 1.44, and 1.60. Here l_r is the length of the roller. We see that in all three cases, $\tau/\rho u_0^2$ (where u_0 is the inflow velocity) varies the same way over the length of the roller.

Another set of bounds for ω near the surface are related to the flow conditions at the toe of the roller. As indicated in Fig 3 in the immediate neighborhood of the toe, the free surface and the dividing streamline can both be approximated by straight lines so that the roller height e in that region increases linearly with distance x_t from the toe ($x_t = x - x_{toe}$). Since the particle velocity in the wave

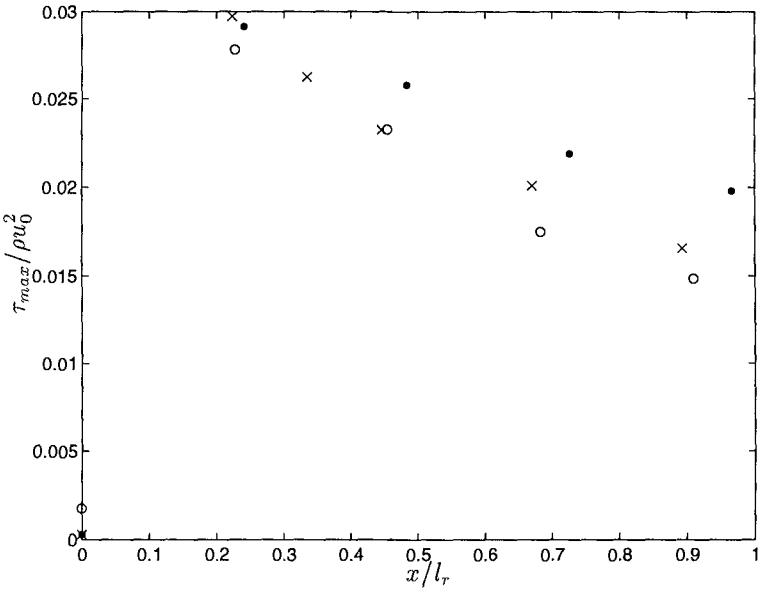

Figure 2: Variation of the maximum shear stress normalized by the square of the inflow mean velocity for three different hydraulic jumps with Froude numbers of 1.28 ('o'), 1.44 ('•') and 1.60 ('×').

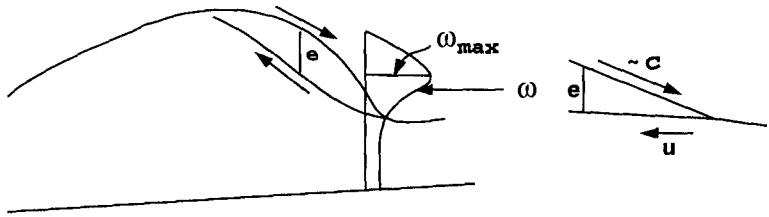

Figure 3: Schematic diagram showing the distribution of vorticity and the approximation at the toe of the roller.

at the surface of the roller is $\sim c$ and at the dividing streamline is $u \ll c$ (where u is close to the velocity in the wave trough) the vorticity ω must vary as

$$\omega \approx \frac{c+u}{e} \tag{20}$$

For dynamic reasons, however, we must also have in that region

$$\tau \propto \rho g e \propto x_t \tag{21}$$

which according to (19) implies that near the toe

$$\nu_t \approx \frac{\tau}{\rho\omega} \propto e^2 \approx x_t^2 \tag{22}$$

Based on the geometry, combined with (19) and measurements of τ and e, we find that ν_t rapidly increases to a maximum value and then decays slowly to near zero before the next breaker arrives.

Based on this information we are able to construct a realistic variation of ν_t and ω_s. We have used

$$\omega_s = A\left(1 - \frac{x_t}{l_r}\right)^2 \qquad 0 < x_t < l_r \tag{23}$$

where l_r is the horizontal length of the roller from the toe to the wave crest, which for dynamic reason must be the rear edge of the roller[2]. For ν_t the relationship is

$$\nu_t = Ch\sqrt{ghe}^{-\beta x_t^2} \tanh^2(\alpha x_t) \tag{24}$$

Though the formulation used in the computations shown in the following are slightly more complicated, the expressions above are similar in effect to those used.

When the boundary condition (17) is applied at $z = \overline{\zeta}$ we get the ω variation shown in Fig 4. Between the $z = \overline{\zeta}$ and the instantaneous MWS it is assumed that ω varies linearly from ω_s to zero at the surface. The hydraulic jump measurements indicate that this is a good approximation to the actual variation.

4. Comparison with experiments

Examples of comparisons with experimental results are shown in the following. The experiments used were obtained by Okayasu and analyzed by Cox et al (1995). Waves were generated in the Precision Wave Tank (PWT) at the Center for Applied Coastal Research at a depth of $0.40m$ and propagated onto a 1 : 35 sloping beach. The measurements were taken at 6 different locations of which some were in the surf-zone. Because a laser-doppler velocimeter was used to measure the velocities, the measurements could only be taken up to a point slightly above the trough level of these waves. Inside the surf-zone, bubble entrainment due to breaking also restricted the measurements.

Figure 5 shows a picture of the model simulations of the waves in the tank at two fixed times. The full line shows the solution of (13) and (14), the dotted line shows the wave transformation without the breaker terms in the equations.

[2]The rapid fluctuations of the toe position imply that at the turbulent averaged mean position of the toe it has a small but finite thickness (Brocchini and Peregrine, 1996). This justifies the finite value of ω_s at the toe in (23)

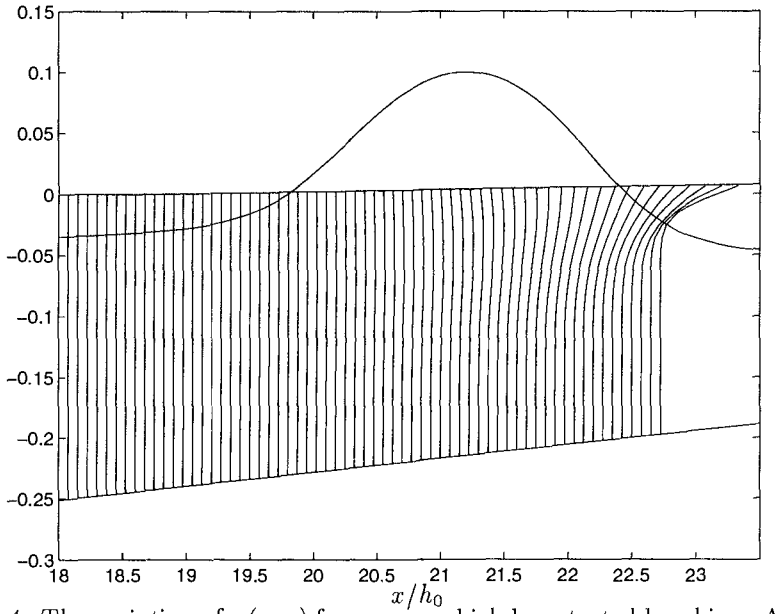

Figure 4: The variation of $\omega(x,z)$ for a wave which has started breaking. Above the MWL, ω varies linearly from the value at the MWL to zero at the MWS.

A comparison with the measured and computed wave heights during the experiment is shown in Fig 6. This figure also shows the measuring positions of the experiment. It turns out that the increase in wave height due to shoaling is slightly underpredicted by the model. In the shown calculation, this has been adjusted for by increasing the input wave height at the left boundary so that the breaker height in this comparison is the same as the measurements. This makes the comparison of the model performance in the surf-zone more relevant.

The underprediction of the shoaling process turns out to be a common feature of the $\zeta - Q$ version of the Boussinesq equations used as the basic Boussinesq model. For comparison we find that if a Boussinesq model based on the depth averaged particle velocity is used, the shoaling is overpredicted slightly. The reason for these inaccuracies and for the difference between the two types of Boussinesq models is that they are both lowest order Boussinesq methods in which terms $O(\delta^2, \delta^3, ...)$ have been omitted. When waves approach breaking, these terms become large enough to influence the solution. The difference between the two model versions appear because the neglected higher-order terms are different in the two versions. Hence, these deficiencies can be eliminated by use of a higher order Boussinesq model (see Wei et al, 1995).

Figure 7 shows a comparison between measured and computed velocity profiles at position L5 which is well into the surf-zone. We see that the agreement is generally acceptable, though it is evident that the lack of measurements near the wave crest makes this comparison less valuable.

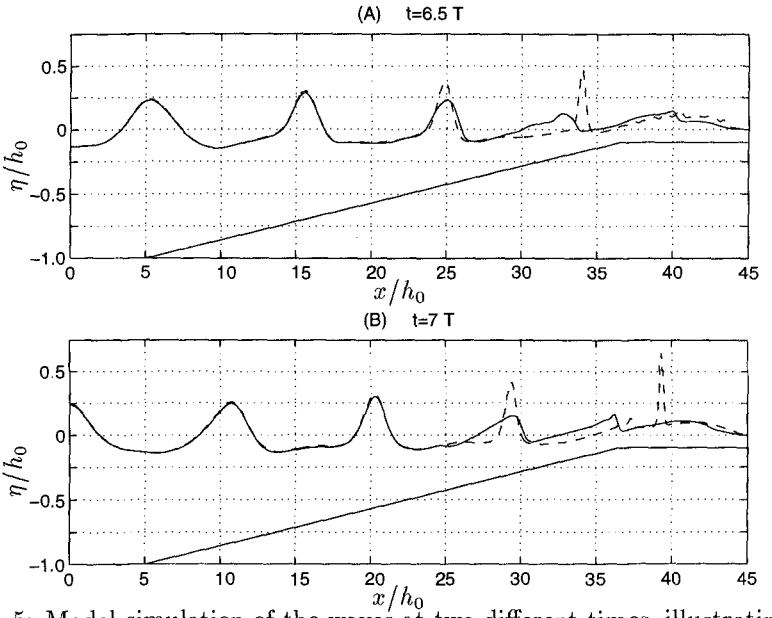

Figure 5: Model simulation of the waves at two different times, illustrating the difference between the non-breaking model (-) and the breaking model (—).

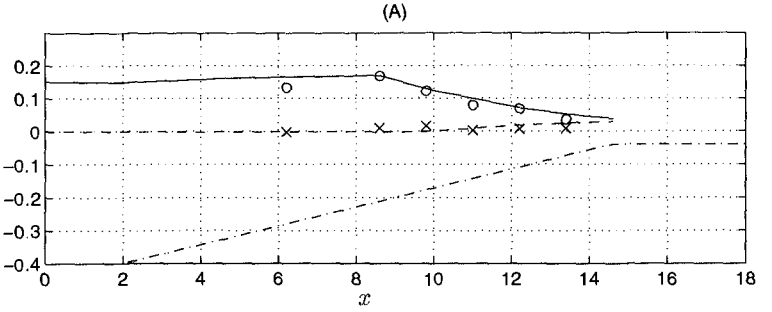

Figure 6: Comparison between the measured wave heights ('o') and the computed wave heights (—) for the experiment described in Cox et al (1995).

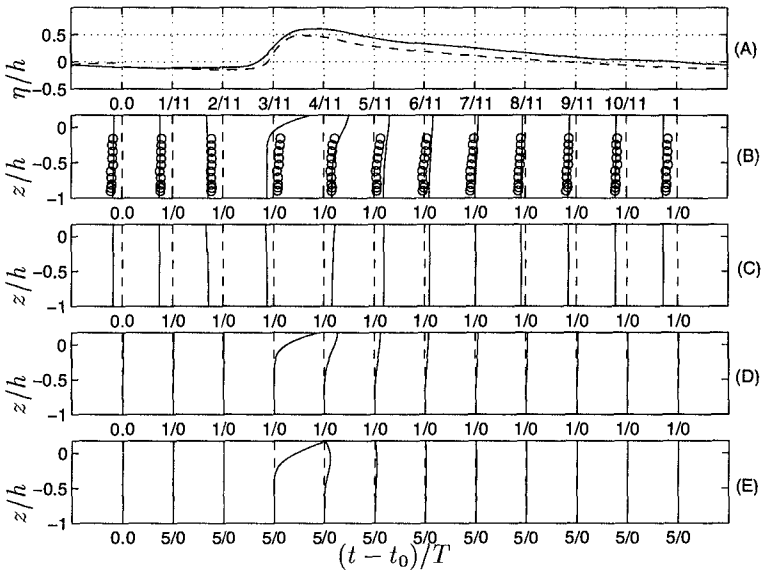

Figure 7: Vertical variations at L5 of: (B) u/c (Solid - Model, Circle - Data), (C) u_p/c, (D)u_r/c and (E) $\omega/(c/h)$ at different phases marked on (A) the surface elevation (solid - Model results, dashed - Data). $t_0 = 7.773\ T$.

Since the effects of turbulence generated by the breaking is included in the model predictions, the average velocity over a wave period should also predict the undertow profiles, which represent a balance in which the shear stresses play a role. Figure 8 shows a comparison between the computed and measured undertow velocities at the 6 measurement positions. Again the agreement is quite good. It is interesting to notice that both measurements and model predictions pick up the principal difference between the undertow under non-breaking waves (parts (A) and (B) in the figure) and breaking waves (parts C-F). Since we have neglected the bottom shear stress, the model predicts a slip velocity at the bottom. It is clear that in the measurements, the effect of the bottom boundary layer is also limited to very close to the bottom.

5. Discussion and comparison with other models

In (13) and (14) the breaker terms are relatively small and it is of interest to see how the strong process of breaking can be properly modelled by adding such seemingly weak modifications.

When solving (13) and (14) the values obtained for Q are actually changed quite substantially. To see this we note that over most of the surf-zone the waves are only changing very slowly. Hence for a given value of ζ we have

$$Q \approx c\zeta \tag{25}$$

which is valid for waves of permanent form with no net mass flux, whether the waves are breaking or not. Therefore, when the wave shape ζ is modified due to

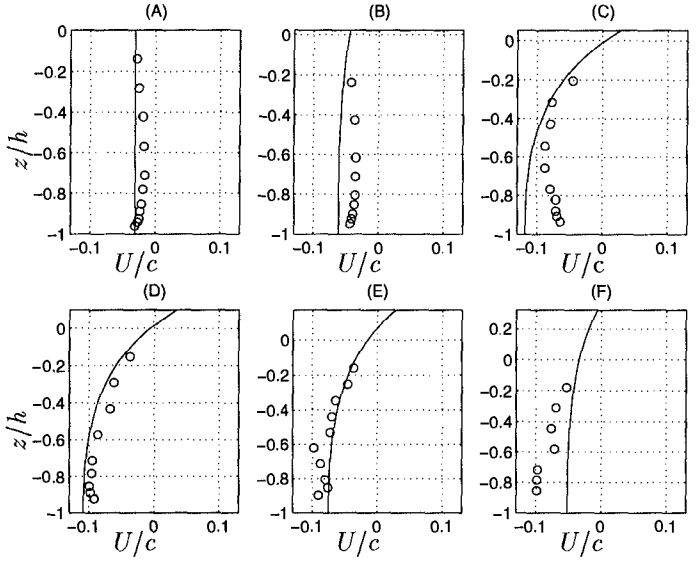

Figure 8: Nondimensional undertow profiles at L1 (A), L2 (B), L3 (C), L4 (D), L5 (E) and L6 (F). (solid) - Model results. (circle) - Data.

the breaking, so is Q.

Even more pronounced is the change in velocity profiles caused by the breaking process. Since Q_r represents a substantial increase in volume flux which is mainly concentrated near the surface it appears that for a given Q the velocity near the bottom must be similarly reduced. This is probably the most significant effect the wave breaking has on the bottom conditions and as the above arguments illustrate, it occurs for simple kinematic reasons[3].

It is also illustrative to examine why several, seemingly quite different, Boussinesq models for breaking waves appear to be comparably good at predicting the wave height decay and surface profile development of breaking waves. In particular, three models show the reduction in wave height and change in skewness of the wave profile towards a sawtooth shape that are typical features of mature surf-zone breakers. The three models in question are the model by Wei & Kirby (1995) which is based on a dissipative term with an eddy viscosity, the model by Schäffer et al (1992) in which the breaking effect is generated by including a surface roller in the model and the present model in which breaking is modelled by taking into account the rotational part of the water motion.

To understand why three so different approaches apparently produce similar effects on the wave profiles, we only need to realize that in the Boussinesq

[3]Another effect of the breaking is the change in the wave profile shape and hence the temporal variation of the pressure gradient and velocities. A third is the added turbulence level even at the bottom.

momentum equation the three models produce almost identical signature of the breaking: the present model and Schäffer et al's model both include two and one terms, respectively, that represent enhancement of the momentum flux. In both models, the (x,t) variation of these terms are approximately the same as shown in Fig 9 (a) and (b). It turns out that, in particular, the position of this momentum enhancement relative to the wave crest is crucial for obtaining the breaking effect. It furthermore appears that in the Wei & Kirby model, the variation of the eddy viscosity has, on a heuristic basis, been chosen so that the "dissipative-term" it creates, in spite of its lack of physical justification, gives an almost identical contribution to the momentum equation. In other words: the Boussinesq equations respond equally to terms that represent the appropriate momentum enhancement, no matter which method are used to determine their variation and magnitude.

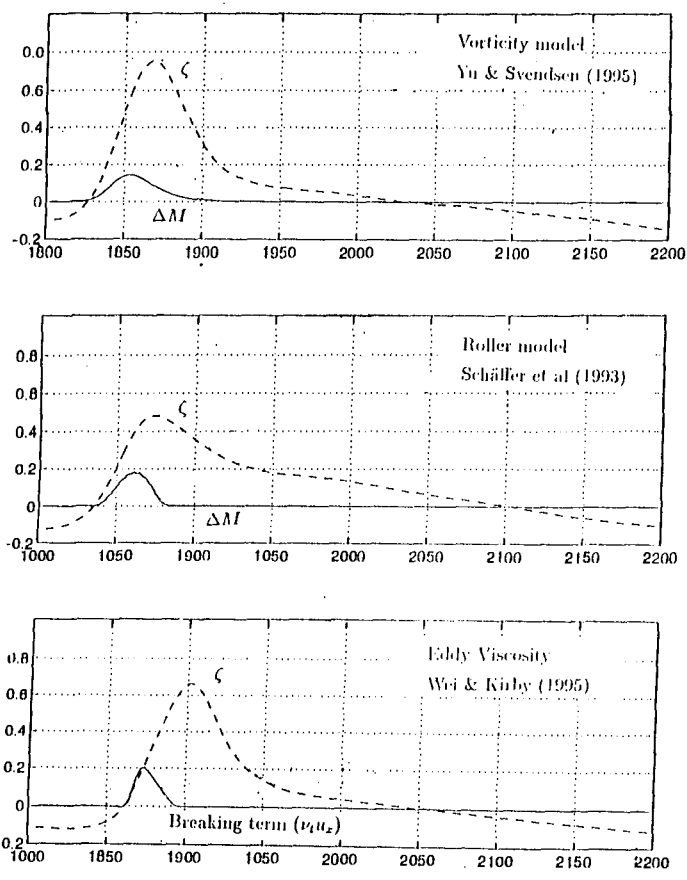

Figure 9: The variation of the terms in the momentum equation which induces breaking, for the three different models discussed in section 5.

6. Conclusions.

The Boussinesq model represents breaking by including the vorticity generated by the breaking. This gives raise to additional terms in the momentum equation which represent the enhanced momentum flux associated with the very large particle velocities at and near the turbulent front of the breaker. The model is based entirely on the Reynold's equations and no artificial dissipation terms are included. It also predicts particle velocities including undertow quite accurately.

Acknowledgment

This study was sponsored by the National Science Foundation under the grant OCE-9203277 and by the US Army Research Office, University Research initiative under contract No. DAAL 03-92-G-0016. The United States Government is authorized to produce and distribute reprints for government purposes notwithstanding any copyright notation that may appear herein.

References

Brocchini,M. and Peregrine, D.H., (1996). "Integral flow properties of the swash zone and averaging" *J. Fluid Mech., 317,* pp.241-273

Brocchini,M., Cherubini, P. and Iovenitti, L., (1991). "An extension of Boussinesq type model to the surf zone." *Computer Modelling in Ocean Engineering 91* , Rotterdam, The Netherlands. pp. 349-359.

Karambas, Th. K. and Koutitas, C., (1992). "A breaking wave propagation model based on the Boussinesq equations." *Coastal Engrg.*, Vol. 18, pp. 1-19.

Lin, J. C. and Rockwell, D., (1994)."Instantaneous structure of a breaking wave." *Phys. Fluids.* Vol 6(9), pp. 2877-2879.

Madsen, P. A. and Svendsen, I. A., (1984). "Turbulent bores and hydraulic jumps.", *J. Fluid Mech.*, Vol. 129, pp. 1-25.

Schäffer, H. A., Deigaard, R. and Madsen, P., (1992). "A two-dimensional surf zone model based on the Boussinesq equations." *Proc. 23rd Int. Coast. Engrg. Conf.*, ASCE, pp. 576-589.

Schäffer, H. A., Madsen, P. and Deigaard, R., (1993). "A Boussinesq model for wave breaking in shallow water." *Coastal Engineering*, Vol 20, pp185-202.

Stive, M.J.F. and H.G. Wind (1982). A study of radiation stress and set-up in the nearshore region. *Coastal Engineering,6*, pp. 1-26.

Svendsen, I.A. (1984a). Wave heights and set-up in a surf-zone. *Coastal Engineering, 8*, pp. 303-329.

Svendsen, I.A. (1984b). Mass flux and undertow in a surf-zone. *Coastal Engineering, 8*, pp. 347-365.

Svendsen, I. A. and Madsen, P. A., (1984). "A turbulent bore on a beach." *J. Fluid Mech.*, Vol. 148, pp. 73-96.

Zelt, J.A., (1991). "The run-up of nonbreaking and breaking solitary waves." *Coastal Engrg.*, Vol. 15, pp. 205-246.